CHEMISTRY OF MATERIALS

Article

Assessment of (*n*,*m*) Selectively Enriched Small Diameter Single-Walled Carbon Nanotubes by Density Differentiation from Cobalt-Incorporated MCM-41 for Macroelectronics

Li Wei, Chun Wei Lee, Lain-Jong Li, Herry Gunadi Sudibya, Bo Wang, Long Qing Chen, Peng Chen, Yanhui Yang, Mary B. Chan-Park, and Yuan Chen

Chem. Mater., **2008**, 20 (24), 7417-7424 • DOI: 10.1021/cm8017677 • Publication Date (Web): 25 November 2008

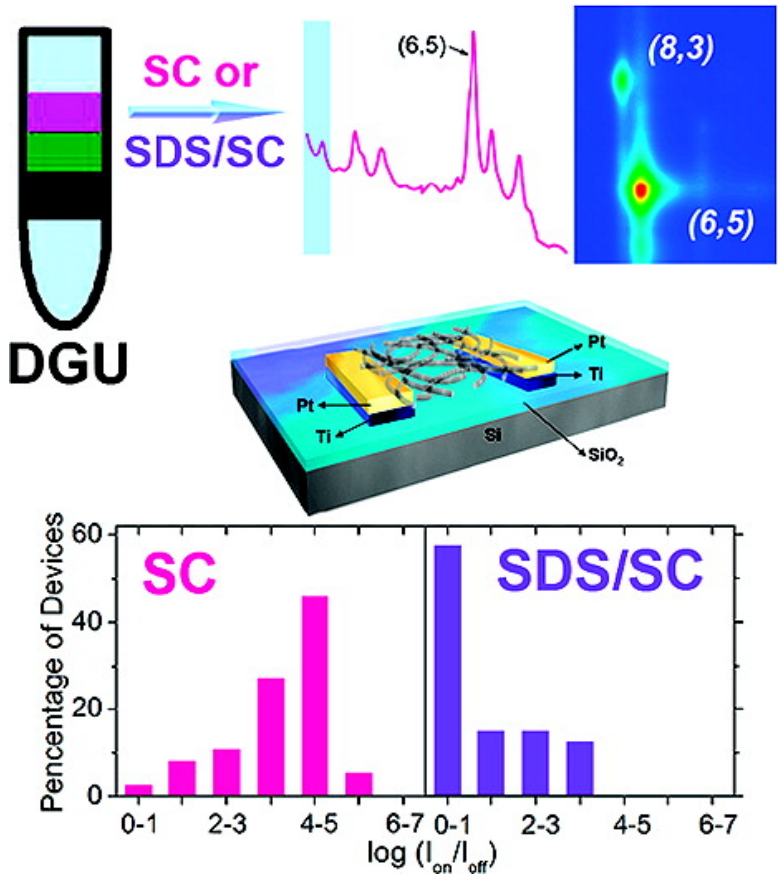

More About This Article

Chemistry of Materials is published by the American Chemical Society. 1155 Sixteenth Street N.W., Washington, DC 20036

Assessment of (*n,m*) Selectively Enriched Small Diameter Single-Walled Carbon Nanotubes by Density Differentiation from Cobalt-Incorporated MCM-41 for Macroelectronics

Li Wei,[†] Chun Wei Lee,[‡] Lain-Jong Li,[‡] Herry Gunadi Sudibya,[†] Bo Wang,[†] Long Qing Chen,[†] Peng Chen,[†] Yanhui Yang,[†] Mary B. Chan-Park,[†] and Yuan Chen*[,†]

School of Chemical and Biomedical Engineering, Nanyang Technological University, Singapore 637459, School of Materials Science and Engineering, Nanyang Technological University, Singapore 639798

Received June 28, 2008. Revised Manuscript Received October 14, 2008

Uniformly semiconducting or metallic single-walled carbon nanotube (SWNT) networks are ideal materials for flexible and large-area electronics (macroelectronics). With the goal of developing optimal enrichment and evaluation solutions toward economical production of monodisperse SWNTs for macroelectronics, we selectively enriched SWNTs, which have small diameters (<0.9 nm) and a narrow (*n,m*) distribution, synthesized on cobalt-incorporated MCM-41 catalysts. The (7,5) enriched SWNTs were obtained from sodium cholate (SC) dispersion, whereas (6,5) were from cosurfactant mixtures of sodium dodecyl sulfate (SDS):SC at 1: 4. Density gradient ultracentrifugation was applied to further refine the separation. Subsequently, SWNT thin-film field effect transistors (FETs) were fabricated using enriched SWNTs. We characterized the chiralities by photoluminescence excitation spectroscopy, optical absorption spectroscopy, Raman spectroscopy, and electrical transport measurements. Among these techniques, results demonstrate that the electrical transport measurement (through I_{on}/I_{off} ratio) of thin-film FETs is the most sensitive technique to evaluate the purity of semiconducting SWNTs. Enriched SWNTs via only SC produced more devices with higher on-/off-current ratios (up to 1×10^6) compared to SWNTs obtained from SDS/SC cosurfactants. These results are different from previous studies using laser-ablation-grown SWNTs (1.1−1.4 nm), encouraging more comprehensive models to explain diameter dependent chirality selection using surfactants.

Introduction

Single-walled carbon nanotubes (SWNTs) have many exceptional electronic properties. [1,2] The use of individual SWNTs as functional elements could be significant for many applications in electronics, optoelectronics, sensors, nanomechanical devices, and other areas. [3−6] However, after 15 years' efforts, realistic applications of devices relied on individual SWNTs are still hindered by their low current outputs, small active areas, and difficulties in integration of individual tube devices into scalable integrated circuits.[7] The emerging applications of SWNTs are based on the two-dimensional network of SWNTs. [7−14] The SWNT network can be regarded as a novel transparent electronic "material" with excellent and tunable electrical, optical and mechanical properties. The SWNT network structures can be printed, making low-cost ink-jet processing possible, and considered to be ideal semiconducting materials for flexible and large area electronics (macroelectronics). Although properties of SWNT networks are expected to be dominated by their percolation paths with the variation among individual tubes being suppressed by the ensemble averaging, the property heterogeneity of SWNTs remains the major challenge in the device development.

As-synthesized SWNTs vary in their diameters and chiral angles, and are characterized by the chiral indices (*n,m*).

* Corresponding author. E-mail: chenyuan@ntu.edu.sg. Phone: (65) 63168939. Fax: (65) 67947553.

[†] School of Chemical and Biomedical Engineering, Nanyang Technological University.

[‡] School of Materials Science and Engineering, Nanyang Technological University.

(1) Dresselhaus, M. S., Dresselhaus, G., Avouris, P., Eds. *Carbon Nanotubes Synthesis, Structure, Properties, and Applications*; Springer: Berlin, 2001; p 447.

(2) Jorio, A.; Dresselhaus, G.; Dresselhaus, M. S.; Eds., *Carbon Nanotubes, Advanced Topics in the Synthesis, Structure, Properties and Applications*; Springer: Berlin, 2008; p 735.

(3) Kong, J.; Franklin, N. R.; Zhou, C. W.; Chapline, M. G.; Peng, S.; Cho, K. J.; Dai, H. J. *Science* **2000**, *287* (5453), 622–625.

(4) Bachtold, A.; Hadley, P.; Nakanishi, T.; Dekker, C. *Science* **2001**, *294* (5545), 1317–1320.

(5) Chen, J.; Perebeinos, V.; Freitag, M.; Tsang, J.; Fu, Q.; Liu, J.; Avouris, P. *Science* **2005**, *310* (5751), 1171–1174.

(6) Chen, Z. H.; Appenzeller, J.; Lin, Y. M.; Sippel-Oakley, J.; Rinzler, A. G.; Tang, J. Y.; Wind, S. J.; Solomon, P. M.; Avouris, P. *Science* **2006**, *311* (5768), 1735–1735.

(7) Kang, S. J.; Kocabas, C.; Ozel, T.; Shim, M.; Pimparkar, N.; Alam, M. A.; Rotkin, S. V.; Rogers, J. A. *Nat. Nanotechnol.* **2007**, *2* (4), 230–236.

(8) Snow, E. S.; Novak, J. P.; Campbell, P. M.; Park, D. *Appl. Phys. Lett.* **2003**, *82* (13), 2145–2147.

(9) Bradley, K.; Gabriel, J. C. P.; Gruner, G. *Nano Lett.* **2003**, *3* (10), 1353–1355.

(10) Wu, Z. C.; Chen, Z. H.; Du, X.; Logan, J. M.; Sippel, J.; Nikolou, M.; Kamaras, K.; Reynolds, J. R.; Tanner, D. B.; Hebard, A. F.; Rinzler, A. G. *Science* **2004**, *305* (5688), 1273–1276.

(11) Hu, L.; Hecht, D. S.; Gruner, G. *Nano Lett.* **2004**, *4* (12), 2513–2517.

(12) Meitl, M. A.; Zhou, Y. X.; Gaur, A.; Jeon, S.; Usrey, M. L.; Strano, M. S.; Rogers, J. A. *Nano Lett.* **2004**, *4* (9), 1643–1647.

(13) Zhou, Y. X.; Gaur, A.; Hur, S. H.; Kocabas, C.; Meitl, M. A.; Shim, M.; Rogers, J. A. *Nano Lett.* **2004**, *4* (10), 2031–2035.

(14) Kumar, S.; Pimparkar, N.; Murthy, J. Y.; Alam, M. A. *Appl. Phys. Lett.* **2006**, *88* (12).

10.1021/cm8017677 CCC: $40.75
Published on Web 11/25/2008

These structural variations result in striking differences in their electronic behaviors, therefore often lead to low on−off ratios, low effective field-effect mobilities and low yields in macroelectronics.[7] One of the key tasks to realize applications based on SWNT networks is to obtain SWNTs with well-defined structures and electronic properties. A recent review has summarized the progress toward monodisperse SWNTs, which includes strategies from various aspects, such as selective growth, enrichment by selective chemistry, electrical breakdown, electrophoretic separation, chromatography, and ultracentrifugation.[15]

Currently, narrowly (*n*,*m*) distributed SWNTs can be grown from Co/Mo catalysts,[16] Fe/Co catalysts,[17] Fe/Ru catalysts,[18] and Co-MCM-41 catalysts.[19−21] Improved (*n*,*m*) selective enrichments were made by the combination of size-exclusion chromatography and ion-exchange chromatography,[22] density gradient separation, [23,24] and cosurfactant extraction.[25] Analytical techniques, including optical absorbance, photoluminescence excitation, Raman spectroscopy, and atomic force microscopy, have been employed by researchers to demonstrate improvements in SWNT monodispersity.[26] Zhang et al.[26] recently measured field effect transistor (FET) performance using about 15 tubes in a 200 nm device channel to evaluate the chirality separation of DNA functionalized HIPCo SWNTs. However, results from those devices involving a small number of tubes in a short channel may not be suitable for macroelectronics whose channel length can easily go up to tens or hundreds of micrometers. Arnold et al. have made thin-film FET electrical transport measurements for devices fabricated from density-gradient separated laser-ablation-growth SWNTs using co-surfactant mixtures of sodium cholate (SC) and sodium dodecyl sulfate (SDS), and have achieved an on/off ratio of 2×10^4.[23] However, they did not report the electrical transport measurements for smaller diameter tubes (<0.9 nm), which are the most predominant SWNTs produced by chemical vapor deposition (CVD). CVD is a more scalable synthesis approach compared to arc-discharge and laser ablation in obtaining high purity SWNTs economically. The absorption spectroscopy studies in our recent study[25] indicated no separation of metallic and semiconducting tubes using SC/SDS cosurfactant mixtures when small-diameter SWNTs from Co-MCM-41 were used. Hence, we attempt to clarify the enrichment efficiency of density differentiation using more sensitive characterization techniques, with the aim of developing optimal enrichment and evaluation solutions toward the large economical production of monodisperse SWNTs for macroelectronics.

First, we carried out (*n*,*m*) selectively enrichment by cosurfactant extraction. Next, the (6,5) and (7,5) enriched SWNTs were sorted using density gradient separation. Photoluminescence excitation (PLE) spectroscopy, UV−vis near-infrared (NIR) absorption spectroscopy, and Raman spectroscopy were then used to characterize enriched SWNTs. Subsequently, we fabricated SWNT thin-film FETs using drop-cast procedure from (*n*,*m*) enriched SWNTs. Atomic force microscope (AFM) were used to monitor the uniformity of SWNT films in device channels. Electrical transport measurements (through on−off ratio of FET devices) were then employed to assess the purity of semiconducting SWNTs. Finally, correlation between analytical techniques and charge transport measurements was evaluated, together with a discussion of (*n*,*m*) enrichment mechanism.

Experimental Section

Growth, Purification, and Surfactant Extraction. Narrowly (*n*,*m*)-distributed SWNTs were obtained from cobalt-incorporated MCM-41 (Co-MCM-41) catalysts. [19,20,27] The precise control of cobalt reduction and nucleation through the MCM-41 template enable size uniform cobalt clusters for the SWNT structure control in CVD synthesis. [28−30] As-synthesized tubes were purified by a mild, four-step purification procedure using NaOH reflux, HCl wash, and oxidation by 4 mol % molecular oxygen at 500 °C to remove contaminates and obtain bulk low-defect-density SWNTs.[31] Purified SWNTs were enriched following the schematic diagram shown in Figure 1. Sample A enriched in (7,5) SWNTs was obtained by dispersing purified SWNTs in 2 wt % SC (SigmaUltra) water solution, whereas sample B enriched in (6,5) SWNTs was obtained through a cosurfactant extraction process.[25] A 10.0 mg amount of purified SWNTs was dispersed in 10 mL of surfactant solution by sonication using an ultrasonicator (SONICS, VCX-130) at 20 W for 30 min in an ice bath. Cosurfactant solutions were subsequently prepared by dissolving a total of 2 wt % surfactants in a 10% (w/v) iodixanol (60% (w/v) (Sigma) water solution with the weight ratio of SDS (MP Biomedicals) to SC surfactant at 1:4. After sonication, suspensions of samples A and B were centrifuged for 1 h at 50 000 *g* (Hitachi-Koki, CS150GXL) to remove nanotube bundles and nonwrapped tubes.

Density Gradient Ultracentrifuge (DGU). Sample A and Sample B were further sorted by density differentiation following the previously reported procedure.[23] SWNT dispersions of sample A and B were concentrated before insert into a linear density gradient. The SWNT dispersion layer of ~ 3 cm thickness was compressed to a dense black layer of 3 mm. The density of the dense SWNT dispersion was adjusted to that of 25% (w/v) iodixanol

(15) Hersam, M. C., *Nat. Nanotechnol.* **2008**, *3* (7), 387−394.
(16) Bachilo, S. M.; Balzano, L.; Herrera, J. E.; Pompeo, F.; Resasco, D. E.; Weisman, R. B. *J. Am. Chem. Soc.* **2003**, *125* (37), 11186–11187.
(17) Miyauchi, Y.; Chiashi, S.; Murakami, Y.; Hayashida, Y.; Maruyama, S. *Chem. Phys. Lett.* **2004**, *387* (1−3), 198–203.
(18) Li, X.; Tu, X.; Zaric, S.; Welsher, K.; Seo, W. S.; Zhao, W.; Dai, H. *J. Am. Chem. Soc.* **2007**, *129* (51), 15770–15771.
(19) Chen, Y.; Ciuparu, D.; Lim, S.; Yang, Y.; Haller, G. L.; Pfefferle, L. *J. Catal.* **2004**, *225* (2), 453–465.
(20) Chen, Y.; Ciuparu, D.; Lim, S.; Yang, Y.; Haller, G. L.; Pfefferle, L. *J. Catal.* **2004**, *226* (2), 351–362.
(21) Luo, Z. T.; Pfefferle, L. D.; Haller, G. L.; Papadimitrakopoulos, F. *J. Am. Chem. Soc.* **2006**, *128* (48), 15511–15516.
(22) Zheng, M.; Semke, E. D. *J. Am. Chem. Soc.* **2007**, *129* (19), 6084–6085.
(23) Arnold, M. S.; Green, A. A.; Hulvat, J. F.; Stupp, S. I.; Hersam, M. C. *Nat. Nanotechnol.* **2006**, *1* (1), 60–65.
(24) Green, A. A.; Hersam, M. C. *Mater. Today* **2007**, *10* (12), 59–60.
(25) Wei, L.; Wang, B.; Goh, T. H.; Li, L.-J.; Yang, Y.; Chan-Park, M. B.; Chen, Y. *J. Phys. Chem. B* **2008**, *112* (10), 2771–2774.
(26) Zhang, L.; Zaric, S.; Tu, X. M.; Wang, X. R.; Zhao, W.; Dai, H. J. *J. Am. Chem. Soc.* **2008**, *130* (8), 2686–2691.
(27) Ciuparu, D.; Chen, Y.; Lim, S.; Haller, G. L.; Pfefferle, L. *J. Phys. Chem. B* **2004**, *108* (2), 503–507.
(28) Ciuparu, D.; Chen, Y.; Lim, S.; Yang, Y.; Haller, G. L.; Pfefferle, L. *J. Phys. Chem. B* **2004**, *108* (40), 15565–15571.
(29) Lim, S.; Yang, Y.; Ciuparu, D.; Wang, C.; Chen, Y.; Pfefferle, L.; Haller, G. L. *Top. Catal.* **2005**, *34* (1−4), 31–40.
(30) Chen, Y.; Ciuparu, D.; Lim, S.; Haller, G. L.; Pfefferle, L. D. *Carbon* **2006**, *44* (1), 67–78.
(31) Chen, Y.; Wei, L.; Wang, B.; Lim, S.; Ciuparu, D.; Zheng, M.; Chen, J.; Zoican, C.; Yang, Y.; Haller, G. L.; Pfefferle, L. D. *ACS Nano* **2007**, *1* (4), 327–336.

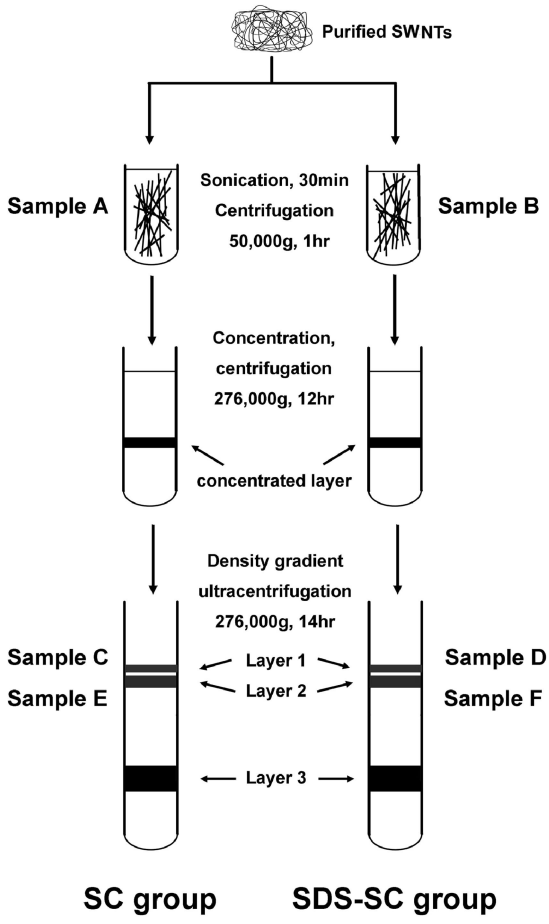

Figure 1. Schematic diagram of the (*n*,*m*) selective enrichment process in this study.

solution (1.132 g/cm^3. Density gradient solutions were prepared by laying 60% (w/v) iodixanol solution with the same surfactant type and concentration as that of SWNT dispersions at the bottom of the centrifugation tube. Then 10% (w/v) ($\rho = 1.086$ g/cm^3 and 30% (w/v) ($\rho = 1.171$ g/cm^3 iodixanol stock solutions were put into two reservoir chambers of a linear gradient maker (SG 15, Hoefer, Inc.) to create a linear gradient layer on top of the stop layer. After the formation of the gradient, the concentrated and density adjusted SWNT dispersion was inserted. DGU was then carried at 276 000 *g* for 14 h. After the DGU, three layers of dispersions with distinctive colors were observed. The upper two layers contain (*n*,*m*) enriched SWNTs, and are close to each other with $\sim$ 0.5 mm (layer 1) and $\sim$ 1 mm (layer 2) thickness. The first layer has a faint pink color, whereas the second layer is of a dark green color. The third broad layer has a black color, containing nonenriched SWNTs, SWNT bundles and other aggregates. The upper two layers with well-defined colors were characterized by spectroscopies, as well as utilized for SWNT thin film FET fabrication.

Characterization of SWNT Dispersion. (*n*,*m*) distribution of SWNT samples were characterized using PLE, UV−vis−NIR, and Raman spectroscopy. PLE measurement was performed on a Jobin-Yvon Nanolog-3 spectrofluorometer with an InGsAs detector. UV−vis−NIR absorption was conducted in the transmission mode on a Varian Cary 5000 UV−vis−NIR spectrophotometer using a 10 mm light path quartz cuvette. SWNT dispersions were filtered onto 25 nm mixed cellulose ester membrane (Millipore) to form homogeneous films. Raman spectra were collected directly from SWNT films on a Renishaw inVia Raman microscope with 633 nm (1.96 eV) laser in a backscattering configuration, and on an Alpha 300 (WITec) Raman microscope with 488 nm (2.54 eV) laser in a scanning mode.

FET Fabrication and Characterization. SWNT thin film FETs were fabricated by the drop-casting method. The concentration of all SWNT dispersions (sample A−F) was adjusted by adding surfactant solutions according to their absorption spectra. First, we adjusted the absorbance at 800 nm of SWNT dispersions to approximately 0.002, which corresponds to a SWNT concentration of $\sim$0.006 mg/mL.[32] Next, we used an integrated area of the absorbance between 904 to 1232 nm (belonging to the E_{11} band of small semiconducting SWNTs) as the second criterion to control the SWNT concentration. Finally, SWNT dispersions were dropped on bottom-contact FET devices, where Pt electrodes with Ti as adhesion layer were patterned on the top of SiO_2/Si substrates using standard lithography techniques. The gate dielectrics SiO_2 is 300 nm thick. The geometry of the FET devices is around 8 μm in the source-drain distance and 20 μm in the channel width. Ten μL of SWNT suspensions was added, followed by drying and rinsing of deionized water. To improve the SWNT film uniformity, the devices were heated up when the same amount of SWNT dispersions were dropped in the middle of device channel for each device. The high evaporation rate at heated device surfaces helps to limit the coffee-ring effect.[33] We observed that the dispersion stain is significant larger than the 8 $\times$ 20 μm device channel. This helps to obtain relatively uniform SWNT films in the device channel, because the device channel stays in the center of the stain. All electrical measurements were carried out in ambient using a Kiethley semiconductor parameter analyzer model 4200-SCS. Atomic force microscopy (AFM) was conducted using a MFP 3D microscope (Asylum Research, Santa Barbara, CA) with a cantilever (Arrow NC, Nanoworld) in ac mode. The scan rate was set to 1 Hz at various scan sizes.

Results and Discussion

SWNTs grown from Co-MCM-41 have narrow (*n*,*m*) distribution, which can be observed from the PLE map of SC dispersed SWNTs in part A of Figure 2. The most dominate species are (7,5) SWNTs with diameter of 0.829 nm. As discussed previously,[25] selective enrichment of (6,5) and (8,3) SWNTs can be achieved through extraction by cosurfactant mixtures of SDS:SC at 1:4. Part B of Figure 2 depicts that the dominate species in sample B are (6,5) SWNTs with diameter of 0.757 nm. After DGU, SWNTs dispersed in SC or SC/SDS illustrate similar PLE maps. Peaks of (6,5) and (8,3) SWNTs can be noted in parts C and D of Figure 2, indicating that smaller diameter SWNTs are enriched in the first pink layers of SWNT dispersions. Peaks of (7,5), (8,4), (7,6), and (9,4) SWNTs can be identified in parts E and F of Figure 2, showing that slightly larger diameter tubes are enriched in the second dark green layers. These diameter selective enrichment results are similar to the study using CoMoCAT SWNTs.[23] It is reasonable as SWNTs produced from both CoMo catalysts and Co-MCM-41 catalysts are at the similar diameter range (main species $<$0.9 nm).

The relative PLE intensities can be used to determine the abundance of different semiconducting SWNTs. Previously,

(32) Itkis, M. E.; Perea, D. E.; Jung, R.; Niyogi, S.; Haddon, R. C. *J. Am. Chem. Soc.* **2005**, *127* (10), 3439–3448.
(33) Deegan, R. D.; Bakajin, O.; Dupont, T. F.; Huber, G.; Nagel, S. R.; Witten, T. A. *Nature* **1997**, *389* (6653), 827–829.

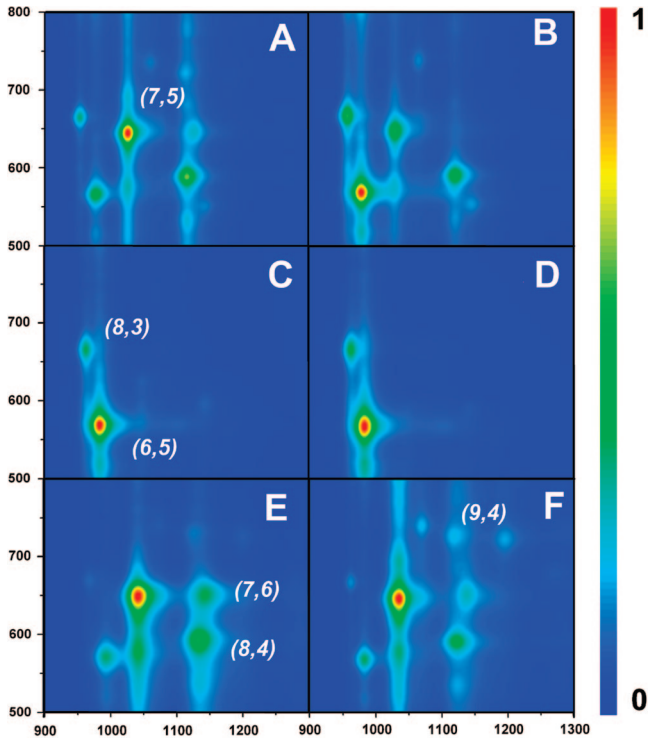

Figure 2. Photoluminescence excitation (PLE) intensity map as a function of excitation and emission wavelength for (*n*,*m*) selectively enriched SWNTs by cosurfactant extraction and density gradient differentiation. Samples A−F were obtained through the procedure as illustrated in Figure 1.

we obtained the abundance by considering the quantum efficiency differences among various (*n*,*m*) tubes based on a single-particle electron phonon interaction model.[31] However, a recent experimental study showed that the quantum efficiency difference among various tubes may not be as large as theoretical predictions.[34] In this study, we directly used the intensity extracted from PLE map to quantify the tube abundance. The results of two most dominant (*n*,*m*) species ((6,5) and (7,5)) were listed in Table 1. The complete sets of abundance analysis data were available in Table S1 to S6 of the Supporting Information. In sample A, the (6,5) to (7,5) abundance ratio is only 0.41. After cosurfactant extraction, the (6,5) to (7,5) ratio increases to 1.83, indicating significant enrichment of (6,5) SWNTs. Results also reveal that the DGU is very effective in enriching smaller tubes. From sample A to sample C, the (6,5) to (7,5) ratio increases 30 times to 12.49; whereas from sample B to sample D, the ratio increases 13 times to 23.90. Samples E and F present the similar abundance distribution as that of sample A.

Effective separation of semiconducting and metallic tubes is a critical step in deciding whether SWNT-based macroelectronic devices will perform to the required specifications. PLE is very sensitive to characterize semiconducting SWNTs, but metallic SWNTs do not present in PLE. UV−vis-NIR spectra have been employed to provide information about metallic tubes in many studies. [23,26] However, it is difficult to obtain such information on metallicity separation for small diameter tubes (<0.9 nm). As illustrated in Figure 3, the lowest absorption E_{11} peaks for all small metallic SWNTs are overlapped below 500 nm with high-energy absorption background that is associated with either the SWNT π-plasmon oscillation or carbonaceous impurities. No changes can be observed for all six samples; therefore, tracking any absorption peak of a specific metallic tube as an indicator of enrichment is not feasible. On the other hand, the selective enrichment of various semiconducting tubes is present in UV−vis-NIR spectra. As shown in Figure 3, both E_{11} (the lowest semiconducting band) and E_{22} (the second lowest semiconducting band) indicate the consistent enrichment trend as that observed in the PLE analysis.

Raman spectroscopy is also commonly used to distinguish metallic and semiconducting SWNTs through the following two features: (1) the lower frequency G-band for metallic tubes has a Breit−Wigner−Fano line shape, which is broader and downshifted in frequency from semiconducting tubes of similar diameter; (2) whenever the energy of the incident photons matches optical transition energy (subject to selection rules for optical transitions) of particular (*n*,*m*) SWNTs, Raman intensity enhancement in radical breathing mode (RBM) of those particular (*n*,*m*) SWNTs can be expected.[35] We measured SWNT thin films of all six samples using Raman spectroscopy. Typical spectra were presented in Figure 4. As shown in part A of Figure 4, no changes were observed in the G-band feature using 633 nm laser. The line shape in part A of Figure 4 also suggests both samples are enriched with semiconducting SWNTs. D-band features, which contributed by defects on SWNTs or amorphous carbon, are neglectable, indicating the high purity of SWNTs. A sharp single RBM peak indicates the narrow (*n*,*m*) distribution. We also measured samples using 488 nm laser shown in part B of Figure 4, because this laser wavelength is known to have strong resonance with smaller diameter metallic tubes. Slight changes in the G-band features can be observed under 488 nm excitation, suggesting that sample D may have higher concentration of metallic tubes compared to sample A. The relative intensity of the Raman peak at 301 nm (may come from (6,6) tubes, under 488 nm) increases, which could be linked to the enrichment of the metallic species. However, because the enhancement of the relative intensity is quite small and various specific Raman wavelengths are necessary to probe different species in resonance,[35] the Raman spectroscopy may not serve as a simple characterization methodology.

Three spectroscopic techniques have difficulties in characterizing metallic SWNTs presented in our enriched samples. We reason that these samples are already highly enriched with semiconducting SWNTs. Metallic SWNTs do exist at low concentration, which make them difficult to be observed in spectroscopic studies. Nevertheless, quantification of small diameter metallic SWNTs based on our spectroscopy data was not feasible, for which we carried out electrical transport measurements as described below. Because of their nearly one-dimensional and defect-free electronic structure, the electron transport in individual semiconducting SWNTs manifests superior field-effect behavior.[1] However, SWNT thin film FETs have significant lower mobility and on/off ratio. High on/off ratio could be obtained if low density

(34) Tsyboulski, D. A.; Rocha, J.-D. R.; Bachilo, S. M.; Cognet, L.; Weisman, R. B. *Nano Lett.* **2007**, *7* (10), 3080–3085.
(35) Dresselhaus, M. S.; Dresselhaus, G.; Jorio, A. *J. Phys. Chem. C* **2007**, *111* (48), 17887–17893.

Table 1. Abundance of Two Main (*n*,*m*) Species Determined From PLE Map Depicted in Figure 2

	A		B		C		D		E		F	
(*n*,*m*)	(6,5)	(7,5)	(6,5)	(7,5)	(6,5)	(7,5)	(6,5)	(7,5)	(6,5)	(7,5)	(6,5)	(7,5)
abundance (%)	14.27	34.90	34.67	18.95	57.13	4.57	62.46	2.61	13.91	41.44	15.22	36.15
(*6*,*5*)/(*7*,*5*)	0.41		1.83		12.49		23.90		0.34		0.42	

networks below the metallic percolation threshold are applied.[36] With the increase of metallic tube concentration, metallic tubes in SWNT networks can easily form continuous paths to lower the on−off ratio.[8] Ideally, SWNT networks with pure semiconducting tubes can achieve both high on−off ratio and mobility. The purpose of this study is to evaluate the (*n*,*m*) selective enrichment of SWNTs synthesized from Co-MCM-41, rather than to achieve the best performance macroelectronic devices. SWNT thin film FET tests were designed to discern the difference among various (*n*,*m*) enriched samples. Under the same device fabrication and characterization condition, we expect that devices obtained from SWNT samples with higher semiconducting purity can yield better on−off ratios compared to samples containing more metallic tubes.

Part A of Figure 5 shows the schematic drawing of SWNT thin film FETs. SWNT networks lie on the top of Pt electrodes which permit the efficient testing of various SWNT samples. Generally, metallic tubes are easier to form continuous pathways that bridge the source and drain over shorter channels. To achieve higher sensitivity in the detection of metallic tubes, 8 μm in source-drain distance was used instead of 20 μm adopted by Arnold et al.[23] To monitor the SWNT film uniformity in the device channel, we performed detailed AFM characterization of SWNT films. In parts B and C of Figure 5, AFM images show both the Pt electrode and SWNT networks. A 5 × 5 μm^2 scan of SWNT networks in the device channel is presented in part D of Figure 5. The AFM sampling for the network structures on various devices show that the network density in the channel area is around 30∼50 tubes/μm^2. On the basis of our previous results,[37] the variation in on−off ratio caused by the network density difference is relatively not significant (a factor smaller than 5) compared with the difference reported later in this study.

Large contact resistance between electrodes and SWNT networks may dominate FET device performance.[13] A serial of devices with different source drain distances ranging from 2 to 26 μm were fabricated. We measured the network resistance versus the source drain distance for SWNT networks of the same density. Resistances of our devices (8 μm in source-drain distance) have about 10−20% contributions from the electrode/nanotube interface at the contacts, similar as our previous work.[37] At negative gate biases, SWNT networks exhibited similar sheet resistances of about 1 MΩ per square. Typical transfer characteristics ($I_{ds}-V_{gs}$ curves) and current−voltage characteristics ($I_{ds}-V_{ds}$) of semiconducting and metallic SWCNT networks are presented

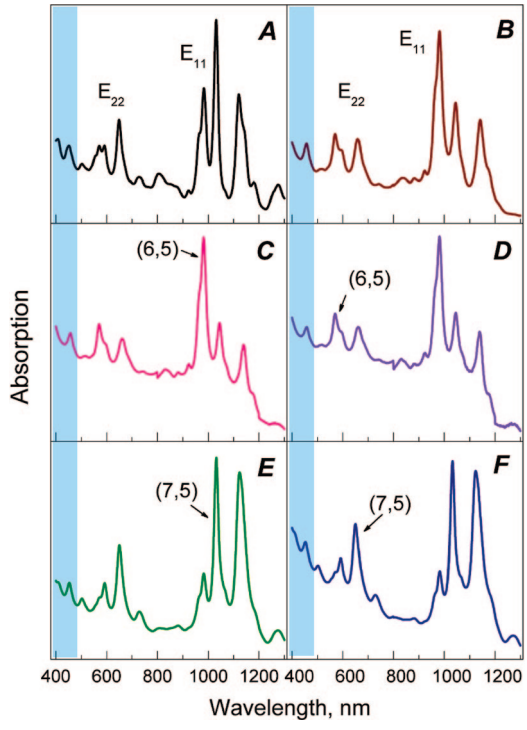

Figure 3. Absorption spectra of (*n*,*m*) selectively enriched SWNTs by cosurfactant extraction and density gradient differentiation. Sample A−F were obtained through the procedure as illustrated in Figure 1. The wavelength range of metallic absorption peaks are shaded in blue color.

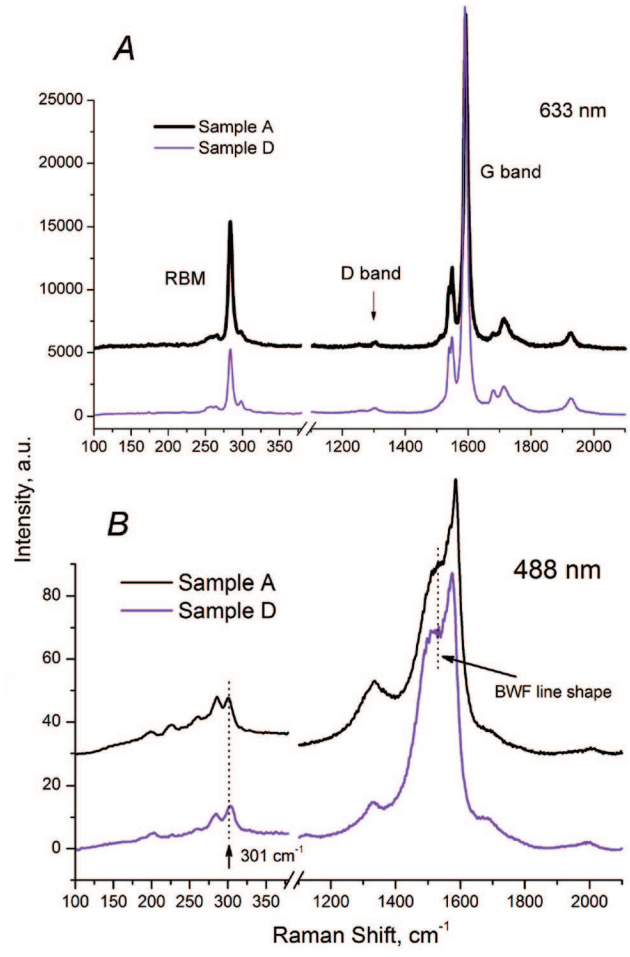

Figure 4. Raman spectra of samples A and D. Spectra of sample A is offset 30% in Y-axis for comparison: (A) obtained under 633 nm laser exciation, (B) obtained under 488 nm laser exciation.

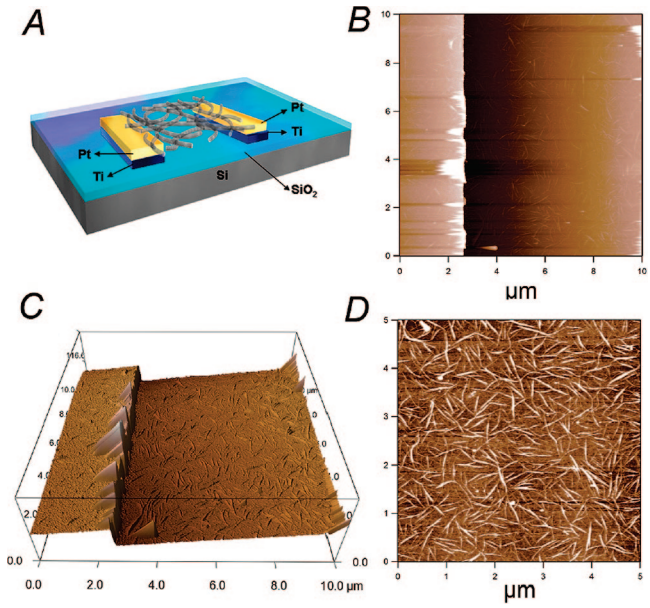

Figure 5. (A) Schematic drawing of SWNT thin-film FETs as described in the Experimental Section. (B)Typical AFM image of a SWNT thin-film device. The left size of the image is the Pt electrode. (C) 3D reconstruction of the AFM image in part B, showing the electrode and SWNT networks in the device channel. (D) Uniform SWNT networks observed in the device channel at a 5 × 5 μm scan.

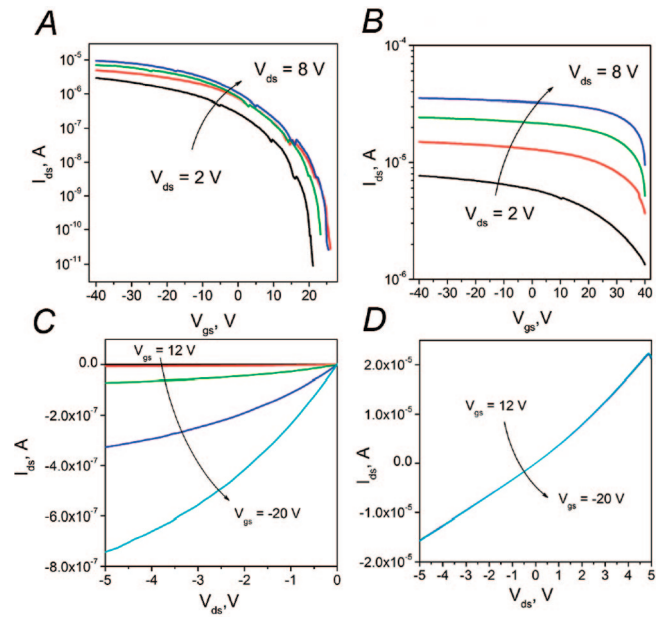

Figure 6. (A) Transfer characteristics ($I_{ds}-V_{gs}$) of a typical semiconducting SWNT device, 54 devices have I_{on}/I_{off} ratio larger than 10^4 in the total 222 measured devices (B) Transfer characteristics of a typical metallic SWNT device, 56 device have I_{on}/I_{off} ratios less than 10 in the total 222 measured devices. (C) Current−voltage characteristics ($I_{ds}-V_{ds}$) of the semiconducting SWNT device at different V_{gs} from 12 V to −20 V with intervals of −8 V. (D) Current−voltage characteristics of the metallic SWNT device.

in Figure 6. When metallic tubes form fewer paths between source and drain, devices exhibit higher I_{on}/I_{off} ratio (parts A and C of Figure 6). On the contrary, when the number of conducting path in SWNT films increases, devices exhibit lower I_{on}/I_{off} ratio (parts B and D of Figure 6). Several other transistor properties for the (*n*,*m*) enriched samples (samples C−F) were listed in Table 2. Property values in Table 2 are the average for the specified number of devices from different SWNT samples (shown in Figure 7). In addition to the on/off ratio differences presented in Figure 7, the effective mobility of devices from samples C and E (with higher on−off ratio) is lower than the effective mobility of devices from samples D and F (with lower on−off ratio). This result is expected and consistent with our previous work.[37] Another observation is that the hysteretic behaviors of devices from samples C and D are more pronounced than those of devices from samples E and F. The details require further investigations. Nevertheless, in this study, we focus on assessing the purity of semiconducting SWNTs by device on−off ratios.

Subsequently, we analyzed different SWNT samples in terms of their device on−off ratio on three aspects: (1) the effect of cosurfactant extraction without gradient differentiation, (2) the effect of DGU, and (3) the difference between SC and SC/SDS cosurfactant assisted DGU. Comparison between part A and part B of Figure 7 suggests that more residue metallic tubes exist in the cosurfactant extracted sample B. No device fabricated from sample B has I_{on}/I_{off} ratio larger than 10^4, while 16% of devices obtained from sample A have I_{on}/I_{off} ratio larger than 1×10^4. Comparison among parts A, C, and E of Figure 7 implies that DGU helps to improve the device performance. Devices from both samples C and E have higher I_{on}/I_{off} ratios, compared to those from sample A. When an individual surfactant (SC) is applied, sample C shows good enrichment of semiconducting tubes with >75% of its devices having I_{on}/I_{off} ratio larger than 10^3. However, such a trend is not found among parts B, D, and F of Figure 7. After SC/SDS cosurfactant assisted DGU, sample D contains more metallic devices, > 70% of its devices having I_{on}/I_{off} ratios less than 100. Difference between samples C and D can also be noted between samples E and F. About 60% of devices from sample E have I_{on}/I_{off} ratio larger than 10^4 compared to 20% of devices from sample F. It should be noted that in Figure 7, the summation of sample C and sample E or sample D and sample F do not match with sample A or B, because after DGU only the upper two layers of dispersions with distinctive colors were extracted for device fabrication, and tubes/bundles in the lower portion of dispersions were discarded.

Spectroscopic studies show that all six samples are enriched with semiconducting SWNTs, yet characterization of SWNT thin film FETs fabricated from those enriched SWNTs reveal that small changes in their semiconducting SWNT purity lead to significant differences in device performance. First, we discuss effects of cosurfactant extraction without gradient differentiation, which include both diameter and metallicity selections. Without gradient differentiation, the enrichment of (*n*,*m*) tubes mainly is caused by the selective absorption of surfactants on SWNTs. Previously, we have shown that the selection of (6,5) and (8,3) tubes (smaller diameter) is optimized when SDS/SC cosurfactant is at 1:4.[25] Although McDonald et al.[38] demonstrated that SDS has a stronger binding to smaller-

(36) Unalan, H. E.; Fanchini, G.; Kanwal, A.; Du Pasquier, A.; Chhowalla, M. *Nano Lett.* **2006**, *6* (4), 677–682.
(37) Lee, C. W.; Weng, C. H.; Wei, L.; Chen, Y.; Chan-Park, M. B.; Tsai, C. H.; Leou, K. C.; Poa, C. H. P.; Wang, J. L.; Li, L. J. *J. Phys. Chem. C* **2008**, *112* (32), 12089–12091.
(38) McDonald, T. J.; Engtrakul, C.; Jones, M.; Rumbles, G.; Heben, M. J. *J. Phys. Chem. B* **2006**, *110* (50), 25339–25346.

Table 2. Average Transistor Properties for (*n*,*m*) Enriched SWNT Samples

sample	I_{off} (A)	I_{on} (A)	threshold voltages forward (V)	threshold voltages reverse (V)	hysteresis ΔV_T (V)	effective mobility($cm^2/(V\ s)$)
C	9.03×10^{-9}	3.57×10^{-6}	20.7	0.6	20.1	1.73
D	1.75×10^{-8}	6.98×10^{-6}	21.4	−0.9	22.2	2.83
E	1.72×10^{-8}	1.02×10^{-6}	16.4	1.7	14.7	0.81
F	6.30×10^{-9}	2.88×10^{-6}	10.8	−1.0	11.8	2.61

diameter nanotubes, we showed that SDS or SC alone has no selection toward smaller tubes.[25] We speculate that the selection to smaller diameter tubes is caused by a particular surfactant shell arrangement of SDS and SC on SWNT surfaces at 1:4, but it remains unclear in precisely which way the surfactant molecules adsorb on the surfaces of SWNTs.[39] In this study, FET device on−off ratios shown in Figure 7 further demonstrates the increase of metallic tube concentration in sample B. The metallicity selection of SDS/SC (1:4) cosurfactant may be caused by the stronger interaction between SC and metallic tubes, because the proximity of the hydroxyl groups in the cholate molecule to the nanotube surface results in electronic polarization toward SWNTs.[38] Metallic tubes have delocalized electrons at the Fermi level, and are more receptive to induced charges.[40] However, it should be noted that metallicity selection is observed only when a mixture of SDS/SC surfactants is used. SC alone (sample A) does not have metallicity selection. Another issue that contributes to the observed metallic tube enrichment is as-synthesized SWNTs at diameter around 0.75 nm may contain higher metallic fractions compared to tubes at larger diameter around 0.81 nm. As shown in Figure 8, the (7,4) tube is metallic sitting right between the (6,5) and (8,3) tubes. We have previously demonstrated that as-synthesized SWNTs are predominately in this same higher chiral-angle region.[41] When smaller diameter (6,5) and (8,3) SWNTs are enriched from sample A to sample B, it is likely that (7,4) tubes or other metallic residues at the similar diameter are also enriched, leading to more metallic tubes in sample B. This is consistent with results obtained from chirality separated DNA functionalized HiPco SWNTs, where more residue metallic tubes exist in the fraction enriched with the (6,5) SWNTs.[26]

Next, what is the effect of DGU? Hersam[15] has summarized that the extent of adsorption of the surfactant on nanotubes of varying chiralities is nonuniform, and creates assemblies with different buoyant densities. This facilitates their separation by isopycnic centrifugation, where particles migrate to regions of like density. DGU sorts SWNTs by their buoyant density leading to layers in the centrifuge tube based on their buoyant density. Nair et al. have proposed a hydrodynamic model to further describe the motion of surfactant-suspended SWNTs in DGU.[40] They suggested that 2.09 and 2.14 SC molecules adsorbed per nanometer along the length of the (6,5) and (7,5) nanotubes respectively. It is easy to comprehend the difference between samples A and E, as well as samples B and F, because large-diameter SWNTs with higher density can be removed by DGU. Removal of large diameter tubes helps to enhance the on−off ratios of devices, as demonstrated in Figure 7.

Nonetheless, it is harder to explain the difference observed between samples C and D, as well as sample E and sample F based on this hydrodynamic model. Although they show almost identical spectra in PLE, absorption, and Raman spectroscopies, devices fabricated from them are significantly different. Samples C and E using SC alone have less metallic residues compared to samples E and F using SDS/SC(1:4) cosurfactant. For smaller diameter tubes (<0.9 nm) in this study, the results are different from those observed for larger tubes reported previously. In the case of laser-ablation-grown SWNTs (1.1−1.4 nm), enrichment of semiconducting tubes were observed at surfactant ratio 1:4, whereas enrichment of metallic tubes were found at surfactant ratio 3:2.[23] If we

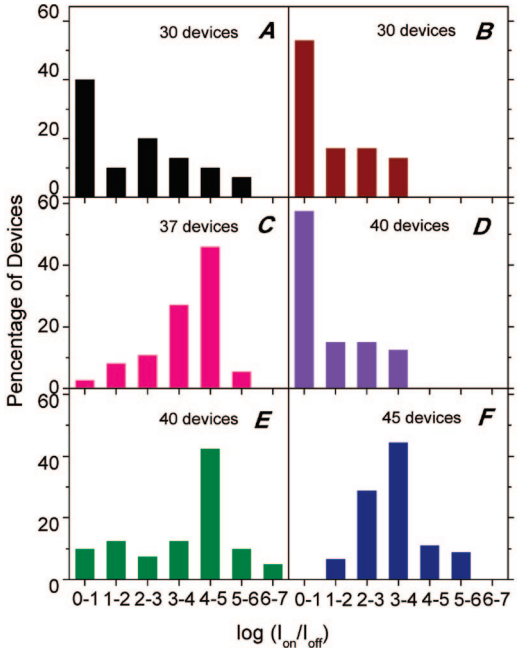

Figure 7. Histograms of device percentages with various on/off current ratios for devices made of (*n*,*m*) enriched SWNTs. A−F correspond to samples A−F as described in Figure 1. The numbers of devices measured for each sample are marked in the figure.

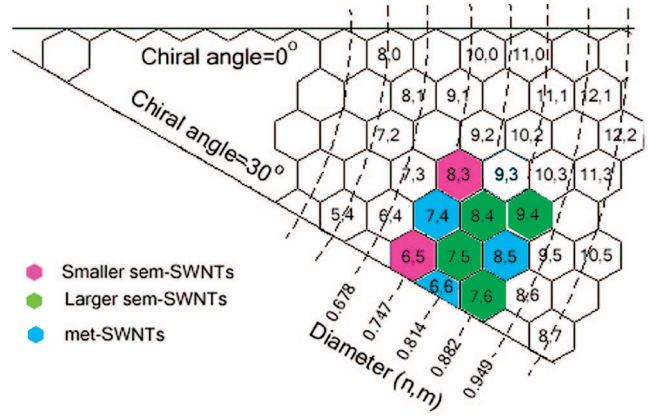

Figure 8. Chirality maps of major (*n*,*m*) SWNT species concerned in this study. Purple hexagons are smaller semiconducting tubes identified in PLE spectroscopy of sample C or D; green hexagons are larger semiconducting tubes identified in PLE of sample E or F. Blue hexagons are possible metallic species that cannot be observed in PLE.

followed the hydrodynamic model,[40] more SC molecules should be adsorbed on metallic tubes such as (7,4) and (6,6). When SC is used alone, the first layer after DGU should be metallic enriched. However, our results in Figure 7 suggest that both samples C and E contain less metallic tubes than sample A. SDS/SC(1:4) assisted DGU also shows better selection to metallic tubes other than semiconducting tubes for smaller diameter tubes. These two results suggest that metallicity selection in DGU is diameter-dependent. To elucidate the observed results, an understanding of molecular level concerning the adsorption of surfactant on SWNTs and dynamics of SWNT-surfactant assemblies in DGU is required. Currently, it is still not available. This study encourages further research on interactions between surfactants and various SWNT species, and such a work is ongoing in our laboratory.

Conclusions

We have performed (*n*,*m*) selective enrichment by both cosurfactant extraction and DGU for smaller SWNTs (<0.9 nm) obtained from Co-MCM-41 catalysts. Even though results from PLE, UV−vis-NIR, and Raman spectroscopy illustrate very similar results among samples, characterization of SWNT thin-film FETs fabricated from those (*n*,*m*) enriched SWNTs reveals that small changes in their semiconducting SWNT purity lead to significant differences in device performance. Cosurfactant extraction (SDS/SC) can enrich smaller diameter tubes, such as (6,5) and (8,3), as well as metallic tubes. Using SC surfactant alone in DGU, higher semiconducting fractions can be obtained from the first two layers; however, more metallic tubes exist in the first two layers when SDS/SC(1:4) cosurfactant is applied in DGU. Electronic transfer measurement of SWNT thin film FETs (by on−off ratio) is more sensitive than spectroscopical studies to assess semiconducting SWNT purity for macroelectronics. The success of SWNT networks in macroelectronics relies heavily on the purity of semiconducting SWNTs similar to the success of Si materials.

Acknowledgment. This work was supported by Nanyang Technological University (AcRF Grants RG38/06 and RG106/06) and Defense Science & Technology Agency, Singapore (MINDEF-NTU-JPP/08/03). We acknowledge AStar SERC Grant (072 101 0020) to P. Chen and M. B. Chan-Park.

Supporting Information Available: (*n*,*m*) abundance analysis of samples from PLE intensity map (PDF). This material is available free of charge via the Internet at http://pubs.acs.org.

CM8017677

(39) Grossiord, N.; van der Schoot, P.; Meuldijk, J.; Koning, C. E. *Langmuir* **2007**, *23* (7), 3646–3653.
(40) Nair, N.; Kim, W.-J.; Braatz, R. D.; Strano, M. S. *Langmuir* **2008**, *24* (5), 1790–1795.
(41) Wang, B.; Poa, C. H. P.; Wei, L.; Li, L.-J.; Yang, Y.; Chen, Y. *J. Am. Chem. Soc.* **2007**, *129* (29), 9014–9019.